PROCEEDINGS OF SCIENCE

SiPM Based Focal Plane Instrumentation Prototype for the MAGIC Telescopes

David Fink[1,2], Alexander Hahn[2], Daniel Mazin[2,3], Jürgen Hose[2], Priyadarshini Bangale[2], Razmik Mirzoyan[2]

[2]Max Planck Institut für Physik, Munich, Germany;[3]University of Tokyo and ICRR, Tokyo, Japan
E-mail: fink@mpp.mpg.de

MAGIC is a system of two 17 m diameter Imaging Atmospheric Cherenkov Telescopes used for gamma ray astronomy. Both the original and the upgraded imaging telescope cameras in use rely on photomultipliers as the photon detectors. In preparation for their possible future use in MAGIC or subsequent telescopes, a camera module with silicon photomultiplier detectors has been developed for operation alongside the existing camera in the telescope. This paper describes front end imaging and electronics challenges and solutions, including the issues of fast analog pulse summation (~4 nsec) of several devices, and the tradeoffs specific to this application's operating environment.

International Conference on New Photo-detectors
PhotoDet2015
6-9 July 2015
Moscow, Troitsk, Russia

[1]Speaker

PoS(PhotoDet2015)006

1.Introduction

MAGIC is a system of two large Imaging Atmospheric Cherenkov Telescopes (IACTs) located on the Canary island of La Palma. The first telescope (MAGIC-I) has been operational since 2004 for scientific observation of very high energy gamma source candidates in the energy range of 55GeV to 50 TeV. A second telescope (MAGIC-II) was installed alongside MAGIC-I, providing stereoscopic mode capability [1]. Both telescopes have a 17 m diameter reflective surface, and are used to measure Cherenkov light from extended air showers [2]. In summer 2012 a new, upgraded camera similar to the one constructed for MAGIC-II was retrofitted in the MAGIC-I telescope [3] (Fig. 1). Each camera pixel has a field of view of 0.1 degrees. Incoming light is concentrated via hexagonal-to-hexagonal reflective light concentrators coupled to the 1 inch diameter hemispherical photocathodes of the photomultiplier tubes (PMTs). Both cameras have a total of 1039 pixels arranged as 169 modules of 7 pixels each. The modules are mounted to an aluminum plate with active temperature control provided by an active closed-loop liquid cooling system. The fast electronic analog signals detected by the camera are converted to an optical analog signal transmitted by means of optical fibers, one per pixel, to a separate building containing readout and trigger electronics.

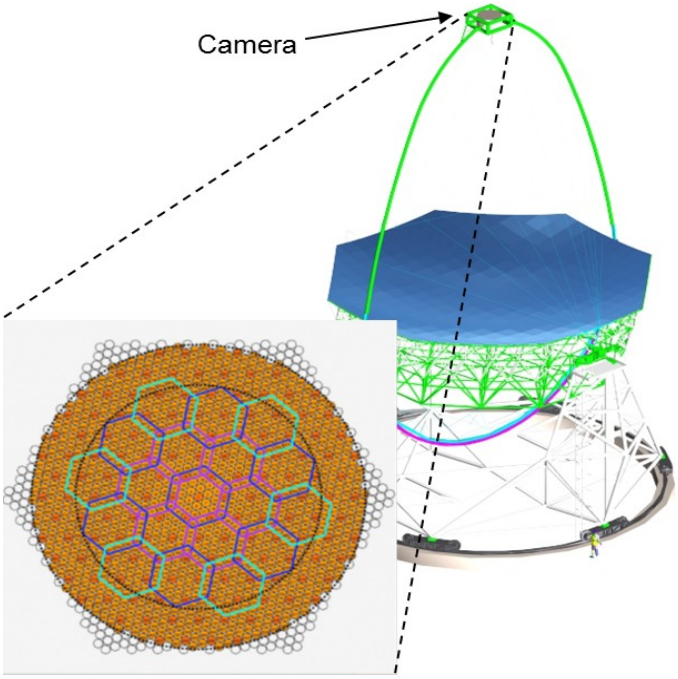

Fig. 1. Location and layout of the camera in the MAGIC telescopes.

2.Operating characteristics of a SiPM based camera module for the MAGIC telescopes

The design of a camera module which uses so-called Silicon Photomultipliers (SiPMs) instead of PMTs as photon detectors must take into account the operating environment seen by the telescope, which differs significantly in some ways from other applications in science or medicine. Issues that must be addressed include the large active detection area needed, the presence of high levels of background light, and operation at near ambient temperatures.

The total camera detector area is dictated by the optical properties of the telescope including field of view, reflector size, and distance of the camera from the reflector. In the case of MAGIC, each individual camera pixel has a hexagonal input aperture area of 780 mm^2. The light concentrators used to direct the incoming light reduce the sensitive area of the photo-detectors needed by a factor of 2 to 3. Commercially available SiPM devices with an area of up to 6x6 mm^2 provide more than the required pixel dynamic range of ~10^3, but do not offer enough sensitive area to cover the output of the light concentrators. Due to this, several SiPMs must be placed adjacent to each other in order to provide sufficient photo-detector area per pixel.

In contrast to many particle physics experiments which operate at low ambient light levels, IACTs are exposed to unidirectional background light known as the night sky background (NSB). The NSB spectrum differs from the Cherenkov signal spectrum measured, providing a potential means of reducing NSB level vs. signal level by matching the spectral response of the camera to the Cherenkov signal. (Fig 2.) However, the SiPM module implemented has a spectral response determined primarily by the spectral response of the devices used. Due to the broader spectral response of the SiPM devices as compared to the spectral response of the PMTs used in the MAGIC cameras, NSB rates from the SiPM module are expected to be higher than the corresponding rates of the PMT based modules. Since the signals are of short temporal duration, a fast signal response is desirable in order to differentiate signal events from the NSB. The PMT modules have a fast response time of 2.4 nsec FWHM to facilitate this.

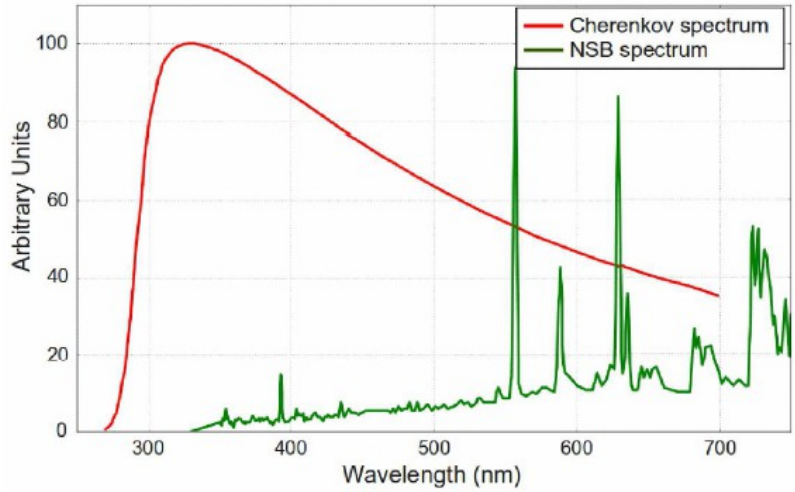

Fig. 2. Cherenkov light and NSB spectrum in La Palma (Canary Islands, Spain) at 2200 m a.s.l., arbitrary units [4].

Two other variable sources of optical background must be considered as part of the design. One is the ambient light from the moon, which depends on the angular separation in the sky separating the object to be observed and the moon as well as the phase of the moon at a given observation time. PMTs degrade over time depending upon the total charge provided by the devices. The SiPM module should not be susceptible to such degradation, making observations at high moon background levels feasible. In addition to the diffuse NSB and moonlight present, the other source of extraneous light is stars in the field of view of the telescope during operation, imaged just in front of the camera focal plane.

3.SiPM module design approach

A side view of a MAGIC camera PMT module is shown in figure 3. Pixels consisting of a light concentrator, PMT with integral Cockroft-Walton high voltage supply, high bandwidth amplifier, and 850 nm optical signal conversion via vertical cavity surface-emitting laser (VCSEL) are housed in 7 individual aluminum tubes. The rearward portion contains the slow control microprocessor and test pulse injection boards, housed in a rectangular enclosure terminated in a bulkhead plate. The connections on the rear bulkhead plate include the optical connectors, power connector, test pulse trigger input, and slow control connector. For compatibility, the physical form factor and rearward mechanical parts remain unchanged in the SiPM module described in this paper. The slow control processor board and test pulse injection board are modified versions of the PMT module hardware.

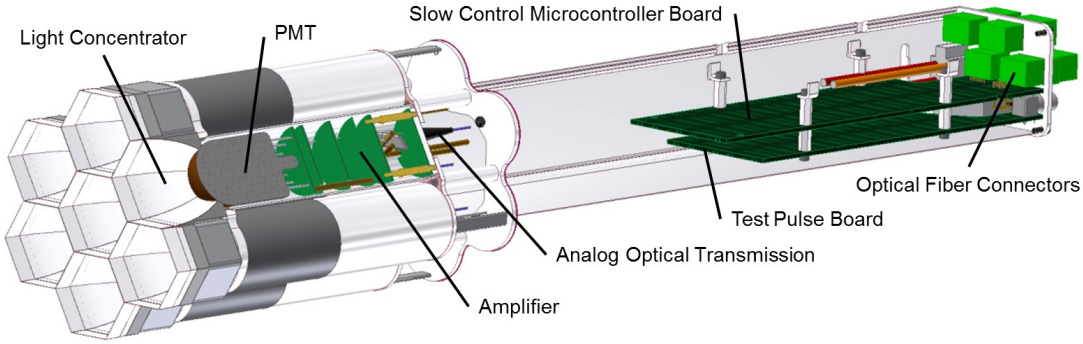

Fig. 3. Side view of the PMT modules employed in the MAGIC cameras.

The light concentrators used for the SiPM prototype are based on modified Winston cones constructed for the MAGIC PMT cameras. The design is optimized for hemispherical PMT photocathodes with a diameter of 1 inch. In contrast, the sensitive surfaces of the SiPM devices are planar. Each concentrator should ideally accept all light coming from the telescope mirror, and reject light from the ground or other objects located adjacent to the mirror surface. The light concentrators were optimized for an acceptance angle of ~30° using the ROBAST simulation program developed for simulating IACT light concentrators [5]. The maximum acceptance angle of the SiPM devices was measured in the laboratory at six separate wavelengths between 309 and 598 nm for both S and P polarization orientations (Fig. 4, 500 nm). An average maximum acceptance angle was taken into account when simulating the combination of light concentrator and SiPM detection plane. The ROBAST simulation results are shown in Figure 5.

4.Sensor type and geometrical arrangement, circuit design

SiPMs are available commercially with several different cell sizes. For this investigation, devices with center-to-center spacing of 50 μm were selected. Larger cell sizes favor better geometrical efficiency. As a consequence, the devices operate at a high gain of ~$1x10^6$. Provided the signals are of short duration, the output current is sufficient to drive the VCSELs used for optical signal transmission over the required dynamic range without the need for further signal amplification. The SiPMs selected for use are Excelitas C30742-66 SiPMs with 6x6 mm^2 area, nominal 100 V bias voltage, and nominal 5 V overvoltage operation.

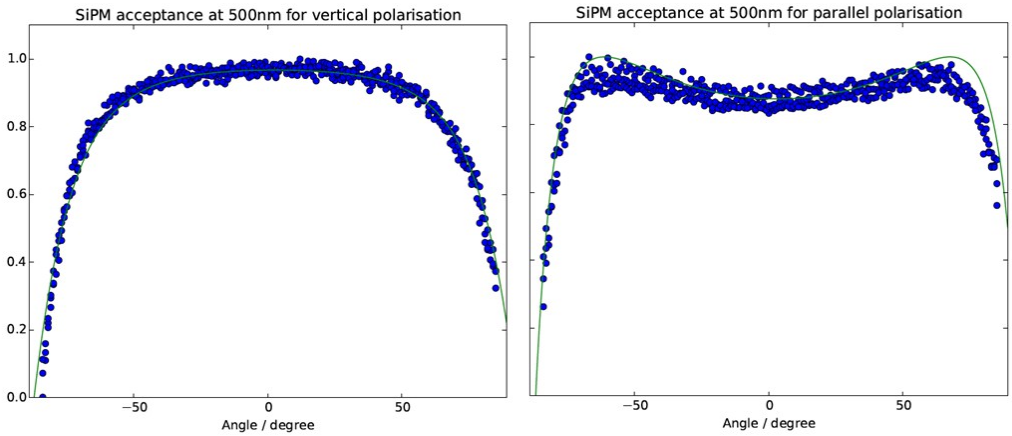

Fig. 4. SiPM acceptance at 500 nm for both polarizations for the SiPM devices used in the prototype module.

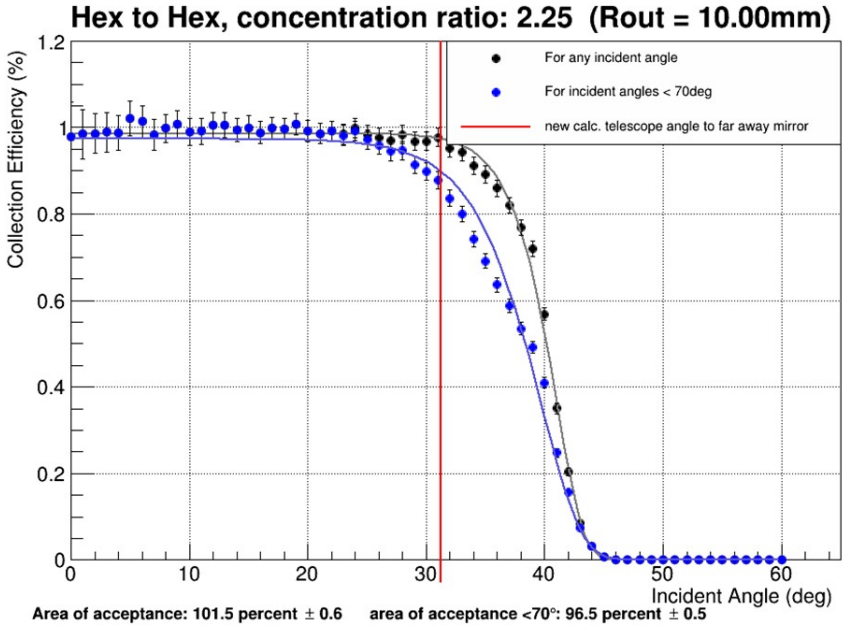

Fig. 5. ROBAST simulation results vs. radial incident angle for light concentrators with light exiting at any incident angle (black) and incident angles <70° as suggested by SiPM acceptance measurements.

Although one square SiPM device with an area of 6x6 mm^2 comprised of 14,400 cells spaced 50 µm apart would be sufficient to cover the desired dynamic range up to 1000 cells fired without geometric saturation effects, the output area of the light concentrators (and thus the required active sensor area) is significantly larger, covering 380 mm^2 in hexagonal form. For the SiPM module, each pixel is configured as an array of 7 sensors comprised of 3 groups of 2, 3, and 2 sensors respectively (Fig.6). Although this configuration does not cover the entire exit area of the light concentrators, the results obtained with this configuration can be geometrically scaled to predict performance with better exit area coverage. Signals of all seven sensors must be summed to form a composite pixel output signal, since reading out each individual sensor would add significant cost while providing no additional information.

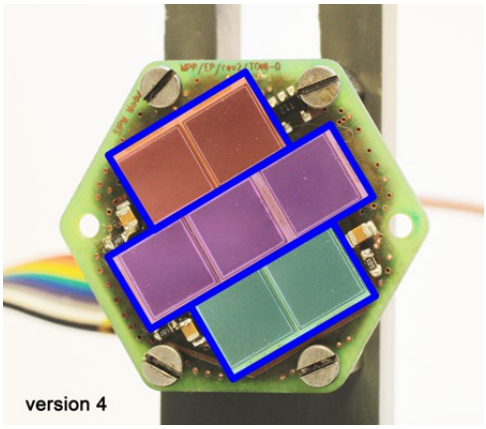

Fig. 6. Spatial arrangement and grouping of the SiPM devices per pixel

The subdivision of the 7 sensors into 3 groups serves several purposes. One is the provision for the application of an individual offset voltage for each group. In this way, the sensors can be sorted by breakdown voltage into subgroups of 2 or 3 devices with similar characteristics. A common bias voltage ranging from 0 to 110 V set via slow control is applied to the SiPM cathode, and an offset voltage individual to each group sets the overvoltage and hence device gain to a uniform level. By applying an offset voltage that reduces the bias across the device to below the breakdown voltage, individual groups can be disabled to lower the signal output level during moonlight operation. If a star is imaged to a pixel, all groups can be disabled to avoid excessive output current and power supply drain.

Several strategies are available for combining the outputs of multiple SiPM devices as a sum of the individual signals. The most straightforward approach would be a common connection at the output terminals of the devices driving a shared load. Unfortunately, this also increases the capacitive load that must be driven depending on the number of devices connected in parallel. This increase in capacitive loading makes it difficult to achieve the short signal timing necessary. Another straightforward approach would be to provide a transimpedance amplifier or similar to isolate each device, and then use a resistive summing network to provide a voltage corresponding to the sum of the individual amplifier outputs. Apart from the complexity and power requirements, such an approach has a negative impact on the noise figure of the composite circuit. A series connection of several SiPM devices in a “totem pole” configuration has been implemented for SiPM sensors used in a low temperature, low rate liquid xenon environment [6]. The advantages of this approach include the reduction of the capacitance to be driven. Disadvantages include resistive losses and high voltages necessary in the bias network, unpredictable operation at high dark count rates associated with room temperature operation, and signal dependence on the level of background illumination (i.e., NSB). For the prototype module described here, a discrete transistor common base current sum circuit has been implemented. The advantages of this approach include low input impedance for fast signal timing, isolation of the device capacitances from each other, and high impedance at the output, allowing the signal current to be summed directly by simply connecting the outputs of the transistors in parallel. The summed current can be used to drive the VCSELs used for optical signal transmission, providing an optical signal proportional to the current sum. A functional diagram of the circuit implemented is shown in figure 7.

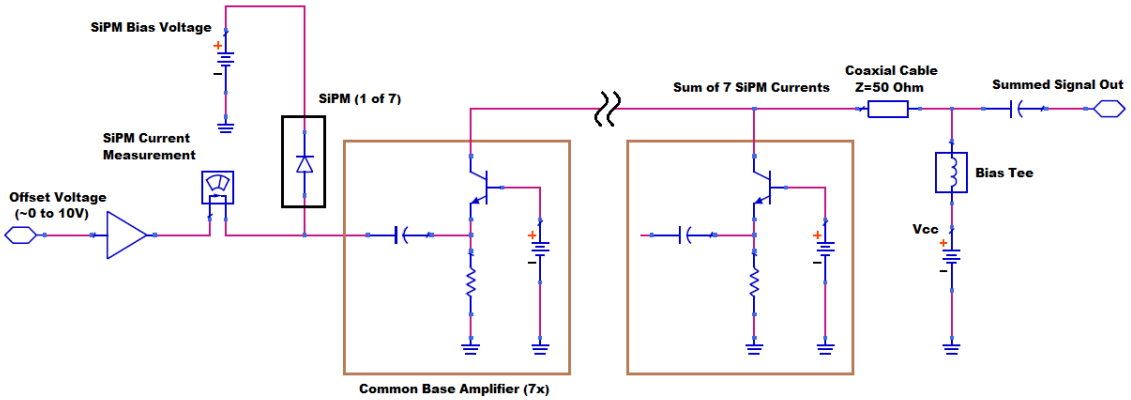

Fig. 7. Functional circuit design of a 7 SiPM pixel including common base summing stage, device current monitoring, and group offset voltage.

Even small SiPM device, transistor package, and circuit board parasitic inductance have a significant impact on the time domain characteristics of the output signal due to the low input impedance of the common base circuit [7]. In order to estimate the influence of the PCB layout, an EM simulator was used to model the PCB layout, and the EM simulation results were included in the circuit simulation model. The implementation uses commonly available BFR92 RF NPN transistors. The nominal operating current is set to 7 mA. The simulation schematic for one sensor is shown in figure 8. Figure 9 compares the time domain simulation results of the summed signals of two SiPMs obtained using the Keysight ADS simulator to the measured summed signal average response of two SiPMs in operation. During design, the SiPM was modeled and simulated as a pure capacitance. Addition of a lumped series inductance of ~5 nH per input to account for device package and PCB trace inductance provides a simulated waveform very close to the measured average waveform.

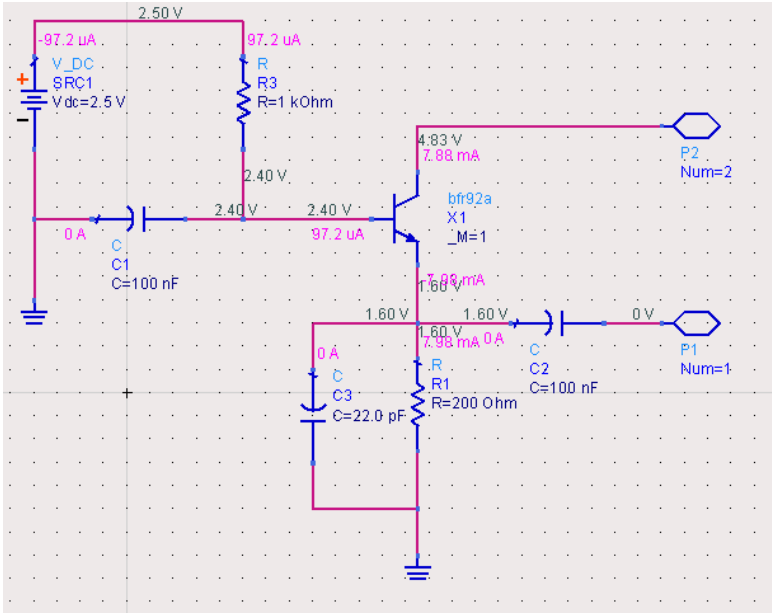

Fig. 8. Common base simulation circuit.

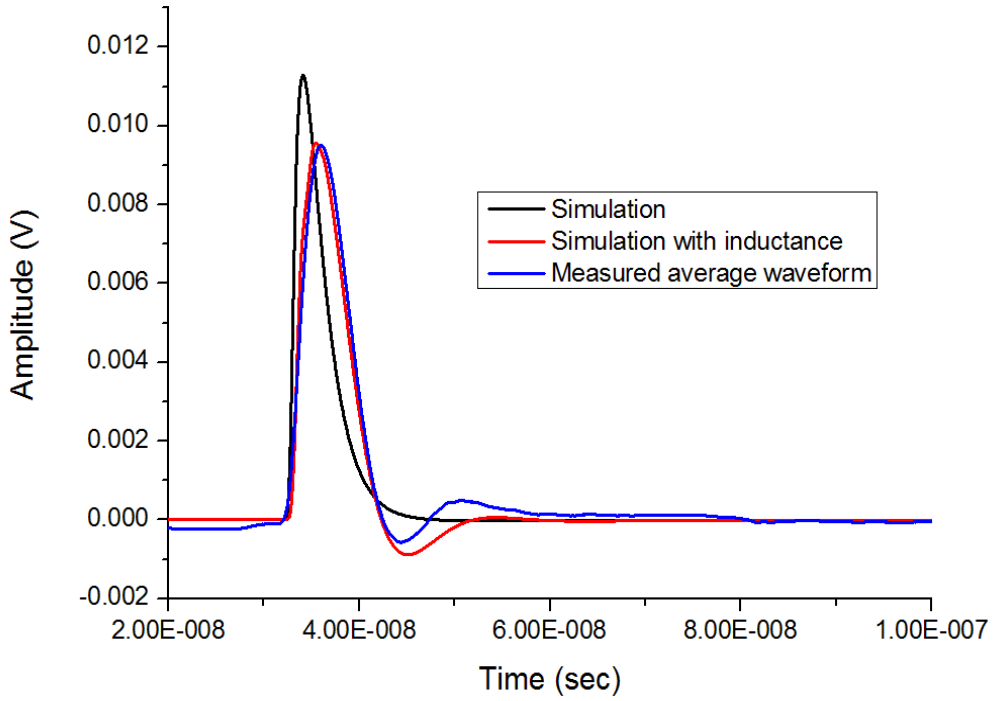

Fig. 9. Simulated (with and without series inductance) vs. measured time domain response, sum of two SiPMs.

5.Implementation, testing, and installation

A cutaway rendering of the front portion of the SiPM module along with images of the actual module and pixel as implemented are shown in figure 10.

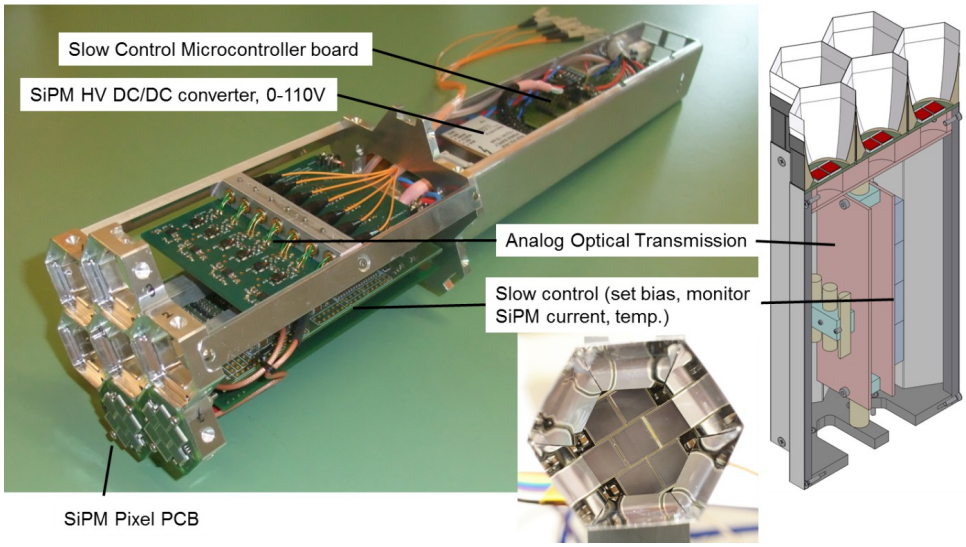

Fig. 10. Cutaway view, partially assembled SiPM module, and SiPM pixel with light concentrator

Measurements of linearity, crosstalk, and single photon resolution were done in the laboratory prior to installation of the module in the camera. An example of a photoelectron

spectrum taken for one sensor group of three SiPMs is shown in figure 11. After laboratory verification, the SiPM module was transferred to the telescope site in La Palma.

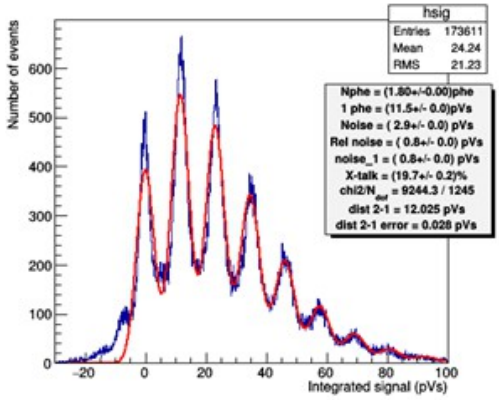

Fig. 11. Sample low light spectrum taken using a pulsed light source for one sensor group (3 devices)

The SiPM module was installed in the middle right corner (as seen from the rear) of the MAGIC I Camera in May 2015 (Fig. 12). A sample event image as recorded by the camera and SiPM module is shown in figure 13.

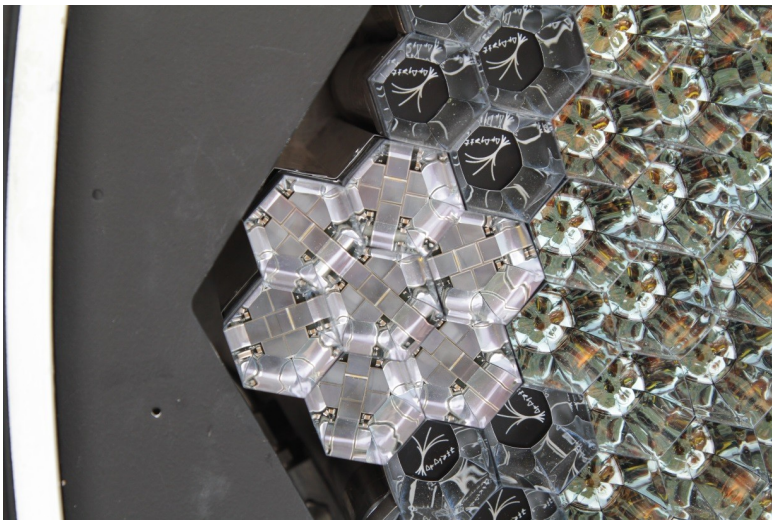

Fig. 12. Close up view of the SiPM module adjacent to the PMT modules in the MAGIC I camera.

6.Conclusions

A first SiPM based prototype suitable for operation in one of the MAGIC cameras has been developed and commissioned. The summation of several device outputs provides adequate detector area per pixel. Subdivision into groups per pixel facilitates adjustment of device gain and adaptation to high background light levels. The common base discrete electronics used to sum the output currents provide fast output signals with a measured FWHM of ~4.7nsec. The SiPM module has been in operation alongside the MAGIC 1 camera since May of 2015.

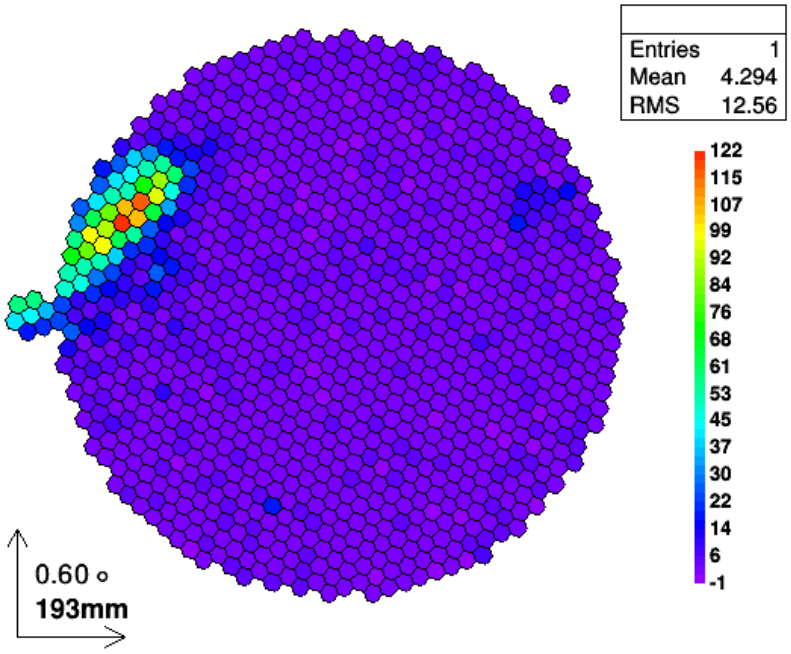

Fig. 13. Sample readout graphic of an event in the camera and SiPM module (to the left of the camera).

References

[1] D.B. Tridon, et al., *Performance of the camera of the MAGIC II telescope*, in: 31st International Cosmic Ray Conference (ICRC 2009), Lodz, Poland, July 7-15, 2009.

[2] E. Lorenz and R. Wagner, *Very-high energy gamma-ray astronomy. A 23-year success story in high-energy astroparticle physics*, The European Physical Journal H, Volume 37, Issue 3, 2012, pp.459-513.

[3] D. Nakajima, et al., *New imaging camera for the MAGIC-I telescope*, in: 33rd International Cosmic Ray Conference (ICRC2013), Rio de Janeiro, Brazil, July 7-15, 2013.

[4] C. R. Benn and S. L. Ellison, New Astron.Rev.,42,503 (1998).

[5] A. Okumura, et al., *ROBAST: Development of a Non-Sequential Ray-Tracing Simulation Library and its Applications in the Cherenkov Telescope Array*,The 34th International Cosmic Ray Conference,30 July- 6 August, 2015 The Hague, The Netherlands.

[6] W. Ootani, et al., *Development of deep-UV sensitive MPPC for liquid xenon scintillation detector, Serial SiPM Circuit*; in: Nuclear Instruments and Methods in Physics Research A 787 (2015) 220-223.

[7] F. Ciciriello, et al., *Interfacing a SiPM to a Current-mode Front-end:Effects of the Coupling Inductance*, IEEE Nuclear Science Symposium & Medical Imaging Conference Seattle, WA USA • 8-15 November 2014.